Spectroscopic Studies on the Interaction of a Water Soluble Porphyrin and Two Drug Carrier Proteins

Suzana M. Andrade and Sílvia M. B. Costa
Centro de Química Estrutural, Complexo 1, Instituto Superior Técnico, 1049-001 Lisboa, Portugal

ABSTRACT The interaction of meso-tetrakis(*p*-sulfonatophenyl)porphyrin (TSPP) sodium salt to human serum albumin and β-lactoglobulin was studied by steady-state and dynamic fluorescence at different pH of aqueous solutions. The formation of TSPP J-aggregates and a noncovalent TSPP-protein complex was monitored by fluorescence titrations, which depend on pH and on the protein nature and concentration. The complex between TSPP and protein displays a heterogeneous equilibrium with large changes in the binding strength versus pH. The large reduction of the effective binding constant from pH 2 to 7 suggests that electrostatic interactions are a major contribution to the binding of TSPP to the aforementioned proteins. TSPP aggregates and TSPP-protein complex exhibit circular dichroism induced by the presence of the protein. Circular dichroism spectra in the ultraviolet region show that the secondary structure of both proteins is not extensively affected by the TSPP presence. Protein-TSPP interaction was also examined by following the intrinsic fluorescence of the tryptophan residues of the proteins. Fluorescence quenching by acrylamide and TSPP itself also point to small changes on the protein tertiary structure and a critical distance $R_0 \approx 56$ Å, between tryptophan and bound porphyrin, was estimated using the long distance Förster-type energy transfer formalism.

INTRODUCTION

In recent years there has been a growing interest in the use of porphyrins and related compounds as therapeutic drugs. They are applied in medicine on important areas as cancer detection and as photosensitizers in photodynamic therapy of cancer (Bonnett, 1995). Potential applications of porphyrins have recently appeared in the treatment of nonmalignant conditions such as psoriasis, blocked arteries, and viral and bacterial infections, including HIV (Ben-Hur and Horowitz, 1995).

Biological effects of porphyrins largely depend on their physicochemical properties, which in turn lead to important changes in their photophysical behavior. In particular, aggregation and axial ligation induce alterations on the porphyrin absorption spectra, quantum yield, fluorescence lifetime, and triplet state lifetime (Uhehara et al., 1993; Tominaga et al., 1997; Togashi and Costa, 2000). Porphyrins are usually introduced in the blood as relatively concentrated solutions, which may diminish its action or even cause adverse effects. Moreover, interactions with macromolecules may control the efficacy and biodistribution of porphyrins, which are known to locate preferentially in the cytoplasm and bind poorly to cell membranes. Therefore, the interaction of these molecules with proteins, especially those that provide carriage through the blood stream, is of utmost importance to formulate safe drugs and effective dosages. In fact, the affinity of some porphyrins for human serum albumin (HSA) binding site II depends on their chemical structure and correlates with the photodynamic efficacy in vivo (Tsuchida et al., 1997).

Water-soluble synthetic porphyrins are structurally simpler than native porphyrin derivatives in the physiological state making easier the interpretation of the structure-function relationship. The aggregation of the anionic porphyrin meso-tetrakis(*p*-sulfonatophenyl)porphyrin sodium salt (TSPP) has been studied extensively. It has been shown that under appropriate conditions, which involve very acidic media and high ionic strength, TSPP forms highly ordered molecular J and H aggregates (Ohno et al., 1993; Akins et al., 1994; Maiti et al., 1995). Very few porphyrins are known to form J-aggregates, the main requisite being the zwitterionic character with the protonation of the pyrrole nitrogen in the macrocycle. More recently, it was reported that these aggregates could also be promoted by interaction with surfactants (Maiti et al., 1998) and proteins (Borissevitch et al., 1996; Huang et al., 1998).

In the present work, we aim to investigate further the interaction of TSPP with carrier proteins, the aforementioned HSA, a transport protein in the blood plasma, which binds to a wide variety of therapeutic drugs, and β-lactoglobulin (βLG). The proper functionality has not been clarified yet, but being also a transport protein interacts with a variety of ligands such as retinol (Dufour et al., 1990) and fatty acids (Frapin et al., 1993) especially through its hydrophobic binding sites even in acid environments. Thus, the proteins sensitivity to pH and the porphyrin aggregation make the study at pH = 2 of physiological relevance.

The binding characteristics were followed by absorption, steady-state, and transient-state fluorescence of TSPP over a large pH range. Because TSPP is a symmetrical molecule, no circular dichroism (CD) signals are obtained. However, they can be induced by the presence of an asymmetric

Submitted August 22, 2001, and accepted for publication October 31, 2001.

Address reprint requests to Suzana M. Andrade, Centro de Química Estrutural, Complexo 1, Instituto Superior Técnico, 1049-001, Lisboa, Portugal. Tel.: 351-21-8419389; Fax: 351-21-8464455; E-mail: sandrade@popsrv.ist.utl.pt.

0006-3495/02/03/1607/13 $2.00

peptide environment bound to the macromolecule as normally occurs in hemoglobins (Ogoshi and Mitzutani, 1998). It is then expected that TSPP-protein complexes present CD spectra, which are useful to understand better the binding process.

The fluorescence of these proteins that arise mainly from the tryptophan (Trp) residues (Trp^{214} in HSA, $Trp^{19}$and Trp^{61} in βLG) show how the relative exposure of the probe varies and may be used to gain information concerning changes in protein conformation upon ligand interaction. Quenching studies involving acrylamide and TSPP itself as quenchers were carried out, and the efficiency of the latter was used to evaluate their location on the protein's environment.

MATERIALS AND METHODS

Sample preparation

NATA (catalog no. A-6501), HSA fraction V, 96 to 99% purity (catalogue no. A-1653), and bovine βLG chromatographically purified and lyophilized ≥90% purity (catalogue no. L-3908) were purchased from Sigma (St. Louis, MO) and used without further purification. TSPP was obtained from Fluka ≥98% purity (catalogue no. 88074) and acrylamide 99% electrophoresis grade (catalogue no. 14, 866-0) from Aldrich (Milwaukee, WI), and both were used as received. The probe concentrations were determined spectrophotometrically considering the molar extinction coefficient $\varepsilon_{280nm}^{HSA} = 42{,}864\ M^{-1}\ s^{-1}$ (Esposito et al., 1999); $\varepsilon_{280nm}^{\beta LG} = 17{,}600\ M^{-1}\ cm^{-1}$ (Barteri et al., 2000); $\varepsilon_{413nm}^{TSPP} = 5.1 \times 10^5\ M^{-1}\ s^{-1}$ at pH 6 (Huang et al., 1998).

Buffer solutions were made up with bidistilled water, following the recommended procedures. In the pH 2 to 7 range, a citrate-phosphate buffer (25 mM) was used. All solvents were spectroscopic grade. In all experiments we used fresh stock solutions of proteins and porphyrin in water.

Apparatus

The pH was measured at 24.0°C with a Crison microph 2002 and the adjustment to the desired pH values accomplished by the addition of HCl or NaOH. A Jasco V-560 spectrophotometer was used in ultraviolet (UV)-Vis absorption measurements. Fluorescence measurements were recorded with a Perkin-Elmer Applied Biosystems (Foster City, CA) LS 50B spectrofluorimeter. Band-pass slits of 7.5 were used for both fluorescence excitation and emission monitoring TSPP, whereas 5.0 slits were used for Trp residues and derivative. The instrumental response at each wavelength was corrected by means of a curve obtained using appropriate fluorescence standards (until 400 nm) together with the one provided with the instrument. Fluorescence quantum yields of aerated solutions of TSPP were determined relative to that of TPP in toluene ($\phi \approx 0.11$) (Figueiredo et al., 1999) with appropriate corrections for the refractive index of the solvent. The quantum yields of Trp in proteins or NATA were determined relative to Trp molecule alone at pH 7 aerated aqueous solution ($\phi = 0.13$) (Andrade and Costa, 2000). Fluorescence decay profiles were obtained by using the time-correlated single-photon counting method (O'Connor and Phillips, 1984) with a Photon Technology International instrument. Excitation was made with the use of a lamp filled with H_2 ($\lambda_{exc}^{TSPP} = 425$ nm and $\lambda_{exc}^{Trp} = 295$ nm) and sample emission measurements were performed until a maximum of 10^4 counts. Data analysis was performed by a deconvolution method using a nonlinear least squares fitting program, based on the Marquardt algorithm. The goodness of the fit was evaluated by statistical parameters (reduced chi-square (χ^2) and Durbin-Watson) and graphical methods (autocorrelation function and weighted residuals).

CD spectra were obtained with a Jasco spectropolarimeter J-720 with spectral averaging and baseline correction. The studies have been performed at a constant TSPP concentration of 2 μM in the visible range and protein concentration was varied (0–7.5 μM for βLG and 0–1 μM for HSA). In the far-UV region the protein concentration was kept constant at 5 μM for both proteins and TSPP concentration was varied (0–20 μM).

All cells used were quartz with 1 cm path lengths, and temperature was maintained at 24.0 ± 0.2°C in a thermostated chamber by using a circulating water bath.

Data analysis

Titration of TSPP with HSA and with βLG

A titration procedure using a fixed amount of TSPP (2 μM) and varying the protein concentration (HSA or βLG) was carried out in buffered solutions at different pH (2 to 7). This titration can be monitored by following the absorbance (Davila and Harriman, 1990a,b) or fluorescence changes (Avdulov et al., 1996) on the TSPP spectra. The binding parameters can be calculated using the Scatchard's equation. This formalism assumes the existence of n ligands binding with equal affinities (for $n = 1$ this equation is similar to the Langmuir isotherm). When there is some cooperativity in the binding process, an equation derived from the Freundlich isotherm (and analogous to the Hill formalism) may be used

$$[TSPP]_b = [TSPP]_{max} \frac{(K[TSPP_f])^n}{1 + (K[TSPP_f])^n} \qquad (1)$$

where b and f subscripts refer to the bound and free TSPP, K is the equilibrium binding constant and if there is cooperativity in the binding process n expresses the system's heterogeneity (if $n = 1$ we have the usual Scatchard's equation). The errors of the calculated parameters were assessed using the error propagation theory and the distribution F of Snedcor was used to confirm with 99% of confidence the relationship among the variables (Lide, 1991).

Acrylamide quenching

Stock solutions of 5 M acrylamide were added as 10 μL aliquots in buffer to 2 mL aqueous solution of 5 μM protein with or without TSPP. Fluorescence emission (F) was measured at 338 nm after 295 nm of excitation (to avoid exciting tyrosyl residues). A correction factor (f_c),

$$f_c = \frac{OD_{total}}{OD_{prot}} \frac{1 - 10^{-OD_{prot}}}{1 - 10^{-OD_{total}}},$$

was applied to F to account for the fact that the quencher absorbs at the excitation wavelength ($\epsilon_{295\ nm} = 0.27 \pm 0.03\ M^{-1}\ cm^{-1}$) (Andrade and Costa, 2000). Quenching data were analyzed using Stern-Volmer equation (Eftink and Ghiron, 1981), $F_0/F = (1 + K_{sv}[Q])e^{V[Q]}$ in which F_0 and F are the fluorescence in the absence and in the presence of the quencher Q, respectively, K_{sv} and V are related, respectively, to the fluorescence extinction rate constant for the dynamic ($K_{sv} = k_q\tau_0$, τ_0 is the fluorescence lifetime in the absence of the quencher) and static processes.

TABLE 1 Absorption and fluorescence emission maxima of TSPP (2 μM) in aqueous solution at different pH in the presence of proteins (HSA and βLG) and in pure solvents ([TSPP] = 4 μM). (λ_{exc} = 425 nm or 518 nm, T = 24.0°C)

Sample	Absorption maxima (nm)								
	Soret (B)		Q_Y (1, 0)	Q_Y (0, 0)	Q_X (1, 0)	Q_X (0, 0)		Emission maxima (nm)	
H_2O (pH 2)	434				593	644.5		674	
H_2O + HSA (0.2 μM) (J-aggregate)	420	489	515	550	591	648	704	655, 718*	718
H_2O + βLG (4 μM) (J-aggregate)	432.5	489			593	645	703	655, 718*	716
H_2O (pH 7)	412.5		515.5	552.5	579	633		645	706
H_2O + HSA (10 μM)	420		516.5	553	592	646.5		653	720
H_2O + βLG (10 μM)	412.5		514.5	551.5	589	646		654	717
Dimethylsulfoxide	419		514.5	550	591	645.5		652	718
Acetonitrile	414		513	546	588.5	644.5		650.5	718.5
Methanol	413		510	545	586	642.5		649.5	716

*Excitation at 490 nm.

TSPP quenching

Similar procedure to that described for acrylamide was carried out using TSPP as quencher. The experimental data were computer-fitted according to the following equation

$$\frac{\Delta F}{F_0} = \frac{(\Delta F_{max}/F_0)[\mathrm{TSPP}]^n}{K_d + [\mathrm{TSPP}]^n} \quad (2)$$

in which ΔF is the change in fluorescence caused upon addition of TSPP, K_d is the dissociation constant, and n is the Hill coefficient (Nelson et al., 2000).

(Förster) Long distance energy transfer

Förster resonance energy transfer is usually expressed in terms of a critical radius, R_0, the distance at which the rate of energy transfer is equal to the reciprocal of the donor fluorescence lifetime and was calculated by the following expression (Lakowicz, 1983)

$$R_0 = 0.2108\left(k^2\phi_f^o n^{-4}\int F(\lambda)\varepsilon(\lambda)\lambda^4 d\lambda\right)^{1/6} \quad (3)$$

with R_0 in Å, in which k^2 is the orientation factor (two-thirds assumed) describing the relative orientation in space of the transition dipoles of the donor (Trp residues) and acceptor (TSPP), ϕ_f^O is the donor quantum yield in the absence of the acceptor, n is the refractive index of the solution, $F(\lambda)$ is the normalized fluorescence spectrum of the donor, $\epsilon(\lambda)$ is the molar extinction coefficient (M^{-1} cm^{-1}), and λ is in nanometers.

RESULTS

Solution properties of TSPP

TSPP is water-soluble and exists as a monomer in aqueous solution below 30 μM shown by the absorption studies. Two chemical forms can be in equilibrium, Scheme 1, due to protonation of the two pyrrolic nitrogen atoms in the porphinato macrocycle ($pK_a \sim 4.8$ at 25°C and $\mu = 0.1$) (Huang et al., 1998).

The absorption spectra of the deprotonated species, $TSPP^{4-}$, exhibits features of D_{2h} symmetry. However, at pH 2 symmetry increases to D_{4h} featuring a shift of the Soret band from 413 to 434 nm and the nonsplitting of the Q-bands (Table 1). In these acidic conditions, two new absorption bands may appear simultaneously at ≈490 and ≈705 nm. These two new bands have been assigned to the formation of J-aggregates in solution and are enhanced by increasing the porphyrin concentration, the ionic strength, and/or the acidity.

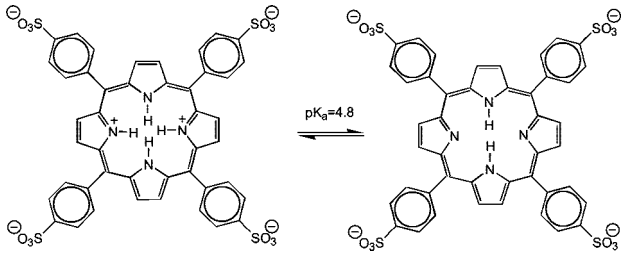

SCHEME 1 Acid–base equilibrium of TSPP in aqueous solution.

At pH 7, $\phi = 0.10 \pm 0.01$ is close to the values found for other free base porphyrins in solvents. Such invariance, found for porphyrins with distinct aryl groups almost orthogonal to the macrocycle plan, must derive from the fact that the π system of the macrocycle is not distorted significantly by changes in the ring peripherical structure. The fluorescence lifetimes agree well with literature data (Table 2). A global analysis treatment of the TSPP singlet state decays was possible and leads to the confirmation of the pK_a for this acid-base equilibrium.

Association of TSPP with proteins in aqueous solution

Titrations of TSPP solutions at a fixed dye concentration (2 μM) and variable protein amounts, HSA or βLG were performed at several pH in the range 2 to 7. The course of the reaction was followed by absorption and fluorescence

TABLE 2 Fluorescence quantum yield and lifetimes of TSPP (2 μM) in aqueous solution at different pH in the presence of proteins (HSA and βLG) and in pure solvents ([TSPP] = 4 μM). (λ_{exc} = 425 nm, λ_{em} = 650 nm, T = 24.0°C)

Sample	Fluorescence lifetimes						Singlet quantum yield*
	A_2	τ_1 (ns)	τ_2 (ns)	τ_3 (ns)	χ^2	DW	
H_2O (pH 2)	–	3.83			1.10	1.65	0.14
H_2O + HSA (1 μM)	0.98	3.83	12.9		1.10	1.65	0.08
H_2O + βLG (4 μM)	0.10	3.76	12.9		1.11	1.89	0.08
H_2O (pH 7)	–			9.8	1.20	1.75	0.10
H_2O + HSA (10 μM)	0.96		12.9	9.8	1.25	1.55	0.10
H_2O + βLG (10 μM)	0.50		12.8	9.8	1.25	1.50	0.11
Dimethylsulfoxide	0.83		12.7	7.0	1.05	1.70	0.04
Acetonitrile	0.74		11.1	6.60	0.94	2.10	0.17
Methanol	0.90		11.2	5.63	1.04	1.99	0.22

*Using ϕ_f = 0.1 for *TPP* in cyclohexane.

spectroscopy. Several changes are detected in the TSPP absorption spectra and are more significant at pH below the porphyrin pK_a. At pH 2, two new bands appear, at [Protein] $\ll$ [TSPP], with exactly the same maxima as those assigned to the J-aggregate (Fig. 1). These bands (490 and 704 nm) increase with protein concentration at the expenses of the Soret band for the first one and of the $Q_x(0,0)$ band for the second one. It seems that the amount of J-aggregate depends on the protein nature. In fact, at [HSA] = 0.01 μM the ratio $OD_{Soret}/OD_{J\text{-}Agg} \approx 2.5$, but the same ratio is only achieved at [βLG] > 0.1 μM.

Noteworthy is the fact that only in the case of HSA, at [HSA] > 0.08 μM, there is a decrease in the $OD_{J\text{-}Agg}$ (at 490 and at 704 simultaneously) and an increase in OD_{Soret} together with a blue shift of this band from 434 to 420 nm. Together with the Soret band blue shift, further addition of HSA leads to the Q band splitting. In the case of βLG, a smaller shift (less than 3 nm) of the Soret band is observed in the protein concentration range used, and the splitting of the Q bands does not take place although a similar red shift of the Q_x bands occur at the same values of dimethylsulfoxide and HSA. The existence of two isosbestic points at 450 and 660 nm leads to the conclusion that the conversion between species is quantitative. Similar values (453 and 661 nm) were found when varying the ionic strength (using KCl) (Akins et al., 1994; Maiti et al., 1995).

The absorption spectra of different species of TSPP present in solution during titration with a given protein are shown in Fig. 2. The conversion of the di-acid monomer ($\lambda_{max}^{Soret} \approx$ 434 nm) to J-aggregates ($\lambda_{max} \approx$ 490 nm) is almost completed when [TSPP] is ~40 times that of HSA and is twice the concentration of [βLG]. J-aggregates become unstable at higher protein concentrations and vanishes when [TSPP]/[HSA] $\approx$ 4:1 and [TSPP]/[βLG] $\approx$ 1:1. At this stage the species with a Soret absorption peak at ~420 nm are stabilized and dominate absorption. So, a similar pattern is followed by the interaction of TSPP with both proteins, except for the fact that higher concentrations of βLG are needed to obtain the same effects as HSA on TSPP.

Curiously, the prominent absorption band at 705 nm is not visible in the excitation spectra, which points to a small

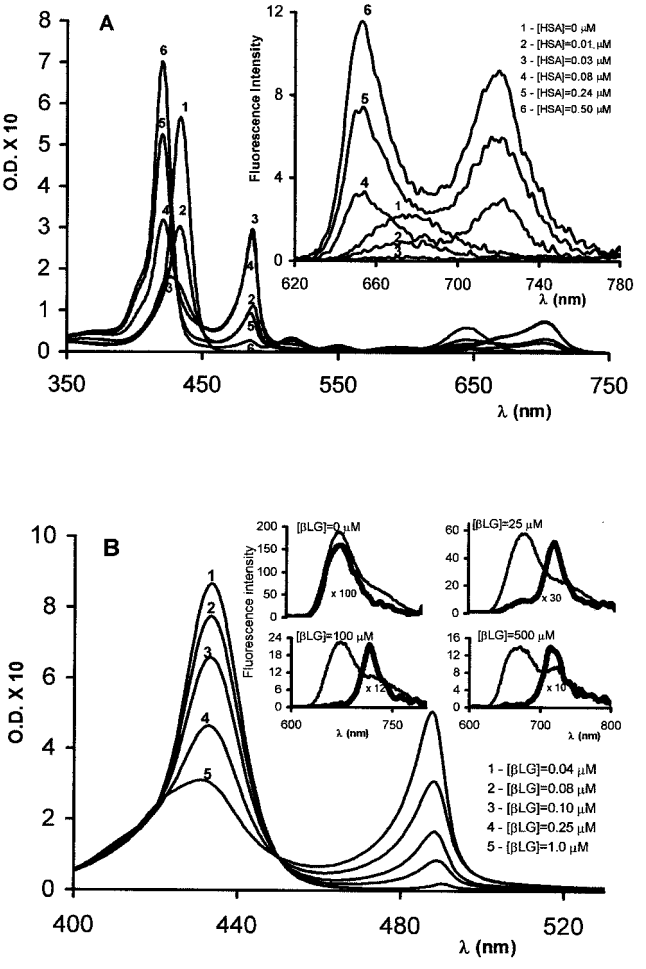

FIGURE 1 Absorption spectra of TSPP in aqueous solution (pH 2) in the presence of increasing concentrations of (*A*) HSA and (*B*) βLG. [TSPP] = 2 μM. (*Insert A*) fluorescence spectra of TSPP at the same HSA concentration range as in absorption (λ_{exc} = 518 nm, T = 24.0°C). (*Insert B*) Fluorescence spectra of TSPP in aqueous solution at pH 2 in the presence of increasing βLG concentration obtained at different excitation wavelength (425 nm, *thin line*; 490 nm, *bold line*)

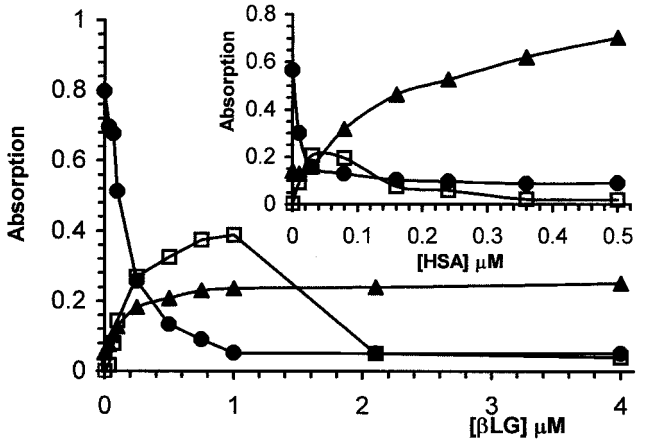

FIGURE 2 Absorption variation of TSPP (2 μM; pH 2) species: di-acid monomer at 434 nm (●), J-aggregates at 490 nm (□), and TSPP/protein complex at 420 nm (▲) during titration with βLG and HSA (*insert*).

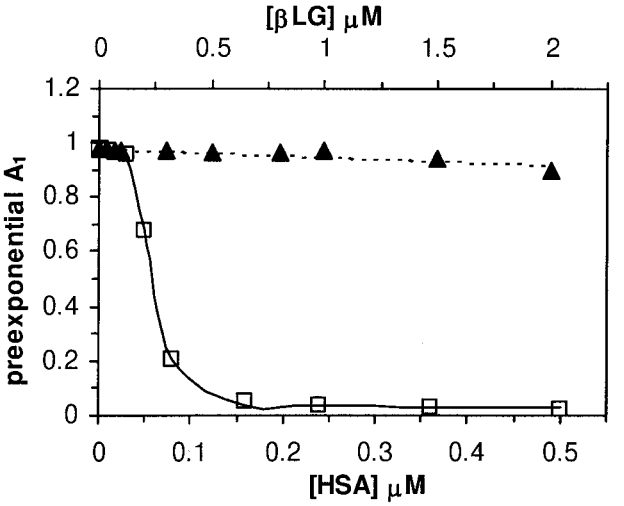

FIGURE 3 Preexponential factors dependence on the protein concentration (□ HSA; ▲ βLG) of the shortest lifetime of TSPP (2 μM) in aqueous solution, pH 2; $\tau_1 = 3.8$ ns and $\tau_2 = 13$ ns ($\lambda_{exc} = 425$ nm, $\lambda_{em} = 650$ nm, $T = 24.0$°C).

Stokes shift for J-aggregate emission. Together with a short fluorescence lifetime (50 ps, Maiti et al., 1995) this suggests that these transitions occur without detectable intramolecular relaxation. At pH 2, in the absence of protein the excitation spectral peaks are in agreement with absorption peaks of the monomer $TSPP^{2-}$ and independent of emission wavelength. The fluorescence obtained upon excitation either at 434 or 580 nm shows a single band with a peak at 674 nm, which is quenched in the presence of protein until [HSA] $\leq$ 0.05 μM and [βLG] $\leq$ 0.5 μM (Fig. 1). When the 490-nm band is dominant, the fluorescence spectra depend upon the excitation wavelength (insert Fig. 1 *b*), which clearly puts into evidence the presence of multiple species in solution. The excitation spectra obtained (data not shown) from emission at 640 nm give peaks at 436 and 595 nm, whereas those from emission at 720 nm show also the peak at 500 nm. In the case of HSA, at concentrations where the shifted Soret band (peak = 420 nm) predominates, fluorescence spectra no longer depend on the excitation wavelength and show two intense bands with maxima at 655 and 720 nm (insert Fig. 1 *a*). These maxima resemble those obtained for TSPP in dimethylsulfoxide, which at this stage seem to confirm a less hydrophilic location for the interacting dye in the protein matrix.

Fluorescence decays of TSPP in the presence of protein were obtained upon excitation at 425 nm and emission at 650 nm and were best analyzed with a sum of two exponentials. A global analysis fitting was attempted, and the results are shown in Fig. 3. The shorter lifetime may be assigned to the dianionic monomer because it is the lifetime value obtained without protein. At these excitation/emission conditions, in the case of HSA, one is clearly monitoring the changes in the population of $TSPP^{2-}$ monomers and in the population of the porphyrin-protein complex. So, the long-lived component $\tau_f \approx 13$ ns may be assigned to that complex. The J-aggregate lifetime is reported to lie in the picosecond domain as mentioned earlier, which is outside the equipment resolution.

The amount of complexed porphyrin is much less in the case of βLG, where J-aggregation itself is promoted, also at higher protein concentrations comparatively to those of HSA, as mentioned above.

Similar studies performed at pH $\leq$ pK_a show a common pattern in the results. In general, J-aggregation promoted by the presence of the protein occurs at higher protein/porphyrin ratios with increasing pH but in a more restricted range. At pH > pK_a, no J-aggregation is detected and the effect of the protein is noticed by the spectral bathochromic shifts, more notorious in the case of HSA, where the maxima are similar to those found at pH $\leq$ pK_a (Fig. 4). The isosbestic point found although not so well defined seems to rule out the presence of other species-like dimers that were detected in the presence of potassium ion and crown ether at pH 9.0 at higher TSPP concentration ($\approx$10 μM) (Maiti et al. 1995). In the present case, checking fluorescence emission, a plot of the area under the spectra versus [HSA] yields a straight line and the decays obtained ($\lambda_{exc} = 425$ nm and $\lambda_{em} = 650$ nm) as will be presented below, do not indicate the presence of other entities apart from the deprotonated monomer and the complex protein porphyrin.

It seems that when porphyrin deprotonation occurs, aggregation is not favored even at high protein concentrations. On the other hand, porphyrin-protein complexation still occurs but at increasing protein amounts with higher pH: e.g., $\geq$0.08 μM (pH 2); $\geq$0.2 μM (pH 3.3); $\geq$0.75 μM (pH 5); $\geq$4 μM (pH 7), in the case of HSA.

Time resolved data also seem to support this type of behavior. Without protein the decays are monoexponentials

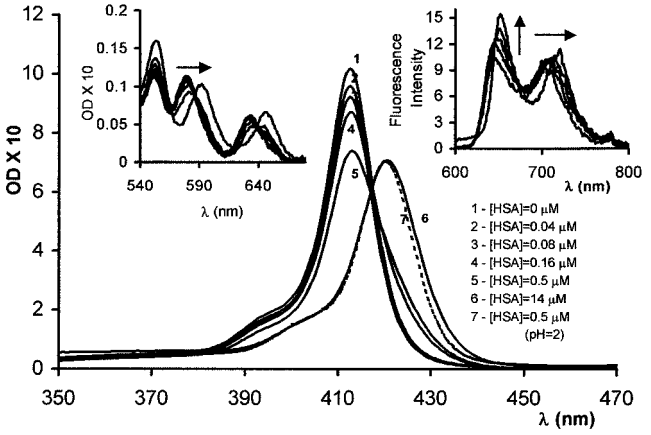

FIGURE 4 Absorption in the Soret band region and of the Q-bands (*insert on the left*), and the fluorescence spectra (*insert on the right*) of TSPP in aqueous solutions of HSA at pH 7 (λ_{exc} = 518 nm, [TSPP] = 1.8 μM, T = 24.0°C).

at pH 7 ($\tau_f \approx 9.8$ ns for the monomeric tetra-anion). However, the presence of the protein induces the appearance of another component ($\tau_f \approx 13$ ns), which is identical to that found at acidic pH and assigned to the complex porphyrin protein. In summary, over the pH range covered there may be three different species detected by fluorescence decays: di-acidic and tetra-anionic monomers of free porphyrin in solution and porphyrin (irrespective of the protonation state) "bound" to the protein (HSA or βLG).

The binding of TSPP to HSA was followed by absorption and fluorescence (steady state and time resolved). A titration procedure using a fixed amount of TSPP and varying the protein concentration was carried out in buffered solutions at different pH. Equilibrium is established between free TSPP molecules and bound to the protein. Using absorption data, it was possible to decompose TSPP Soret band in a sum of three Gaussian functions over the entire pH range covered (Fig. 5 *a*, an example of those fittings is presented in Fig. 5 *b*) at pH 2 and 7. The OD of each component plotted versus the protein concentration shows the growth (at 420 nm) and the decrease (at 413 nm) of the components (insert Fig. 5). These values were used to calculate the associated binding constants.

An attempt to analyze the entire titration curves using the Scatchard formalism failed. A plot of the above equation (n = 1) with our data does not hold because it becomes nonlinear at all pH studied, indicating either that there is more than one class of binding sites or that the binding of each successive molecule alters the association constant of the next molecule (i.e., cooperativity). A similar behavior has been observed previously for binding of hematoporphy-

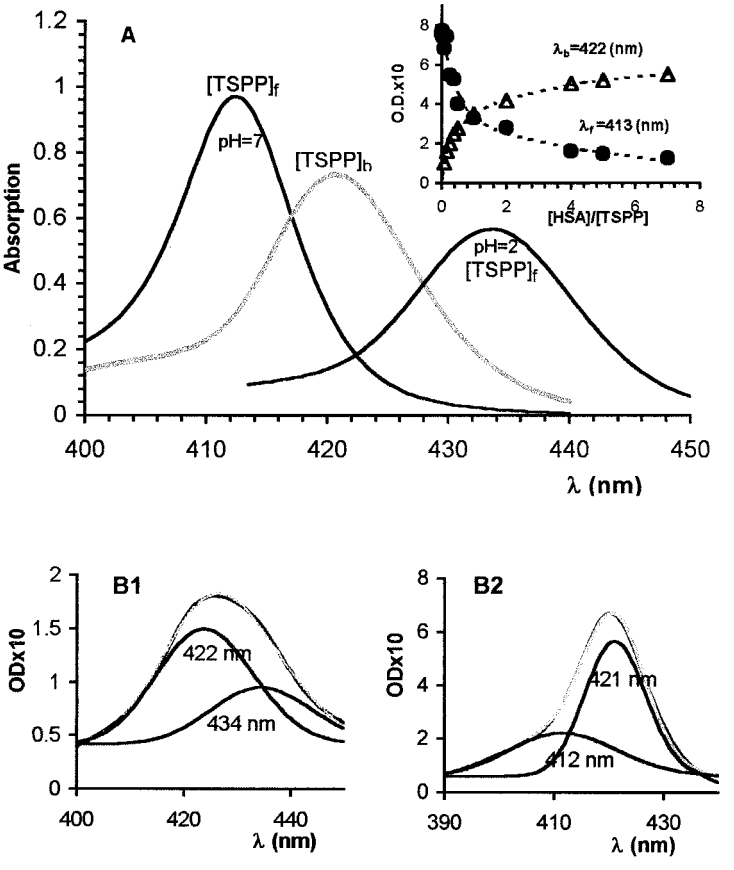

FIGURE 5 (*A*) Absorption spectra representing the different species of TSPP (2 μM) present in aqueous solution at different pH with HSA obtained by Gaussian decomposition of experimental data. ($[TSPP]_f$ stands for the monomeric species di-anion at pH 2 and tetra-anion at pH 7 and $[TSPP]_b$ represents the complexed species). (*Insert*) Absorption dependence on the protein concentration for the two species at pH 7 after decomposition. These data were used to obtain the binding parameters using Eq. 1. (*B*) Example of the fittings obtained for the Soret band decomposition at (*B1*) pH 2, [HSA] = 0.03 μM and (*B2*) pH 7, [HSA] = 8 μM.

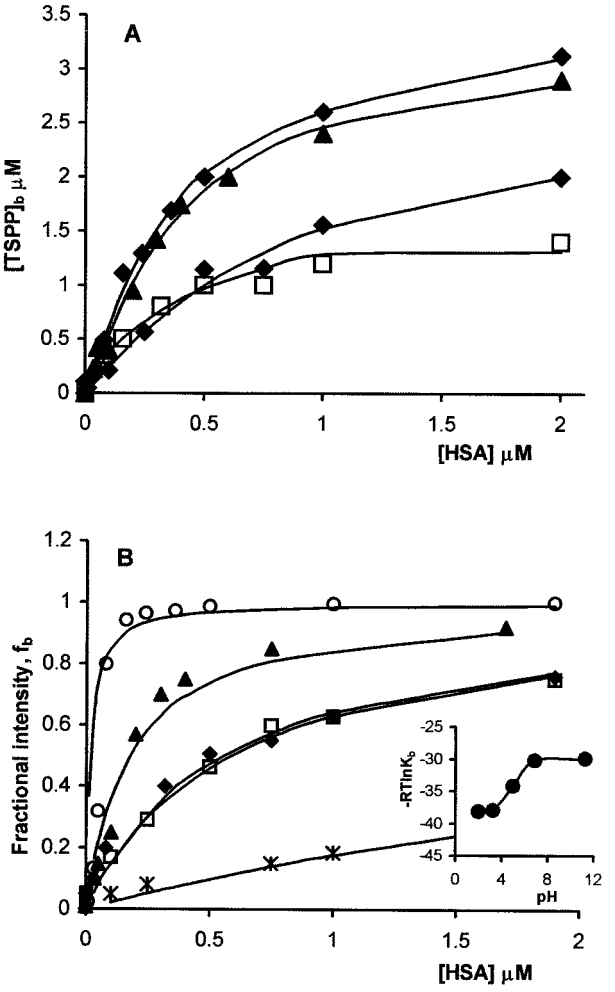

FIGURE 6 (*A*) Plot of the absorption spectral data to Eq. 1 at pH 2 (○); pH 3.3 (▲); pH 5 (♦); pH 6.9 (□). (*B*) Fractional intensities of TSPP fluorescence decays associated with the longest lifetime ($\tau \approx 13$ ns) versus protein concentration at different pH (∗ pH 11, the remaining symbols have the same correspondence as in *A*). The full lines represent best fits with Eq. 4. (*Insert*) Plot of free energies versus pH. The "turning point" of the sigmoidal fit gives a pH 5.2 ± 0.2.

rin derivative (Grossweiner and Goyal, 1984) and a zinc porphyrin (Davila and Harriman, 1990a) with HSA. In some cases a concavity has been detected in such representations and interpreted as indicating the existence of two sets of binding sites where electrostatic and hydrophobic interactions are differently important (Saboury et al., 1996).

To determine the cooperativity in the binding process, Eq. 1 was used. The best fits are shown in Fig. 6 *a*, and Table 3 summarizes the binding parameters obtained and the errors calculated. The value of n is close to 1.4 at pH $\leq$ pK_a of TSPP and below unity ($\approx$0.85) above that pH. The value of K is quite high at all pHs, although it seems to decrease with this parameter, pointing to important electrostatic interactions in the complex.

Time-resolved fluorescence lead also to the same conclusion. The fractional intensity associated to the longest component ($\tau \approx 13$ ns), f_b, should be proportional to the amount of bound TSPP. Using Eq. 4,

$$\frac{1}{f_b} = 1 + \frac{\varepsilon_f}{\varepsilon_b}\frac{\phi_f}{\phi_b K}\frac{1}{[P]} \tag{4}$$

in which ϵ_f and ϵ_b are the extinction coefficients of free and bound TSPP, respectively, and ϕ_f and ϕ_b correspond to the fluorescence quantum yields of those species, a plot of f_b versus the protein concentration allows the estimation of a binding constant at each pH studied, which are consistent with those obtained using absorption data (Fig. 6 *b* and Table 3). Taking $\Delta G = -RT \ln K$, a plot against pH (insert Fig. 7) shows a sigmoidal behavior with a turning point at 5.2 ± 0.2 for HSA, which is similar to the *pI* of the protein.

CD Spectra

TSPP is a symmetrical molecule and does not yield signals in CD spectra at the conditions above studied of pH and probe concentration. However, it tends to show a significant CD signal upon formation of the aggregate in the presence of the protein (Fig. 7) indicating an assymetrical perturbation in the fluorophore. Hemeproteins exhibit characteristic induced CD in the Soret band, reflecting the interaction between achiral porphyrins and chiral proteins. These studies showed that the carbonyl and the OH− group can induce CD in a heme if they are fixed near the porphyrin plane (Ogoshi and Mitzutani, 1998).

TABLE 3 Binding parameters for the interaction TSPP-protein in aqueous solution at different pH obtained by fit of experimental data using Eq. 1

	HSA		βLG	
pH	n	K × 10^{-6} (M^{-1})	n	K × 10^{-6} (M^{-1})
2.0	1.5 ± 0.1	5 ± 2; 5.1 ± 0.4* (0.2 ± 0.1)†	1.2 ± 0.2	3 ± 2 (0.1 ± 0.1)†
3.3	1.2 ± 0.2	2 ± 1; 4.5 ± 0.5*	1.1 ± 0.1	3 ± 2
5.0	1.1 ± 0.1	1 ± 1; 1.1 ± 0.4*	0.9 ± 0.1	1 ± 1
6.9	0.80 ± 0.05	1 ± 1; 0.6 ± 0.1*	0.80 ± 0.05	1 ± 1

*Value obtained using Eq. 4.
†Values obtained from fluorescence quenching of the protein by TSPP using Eq. 2.

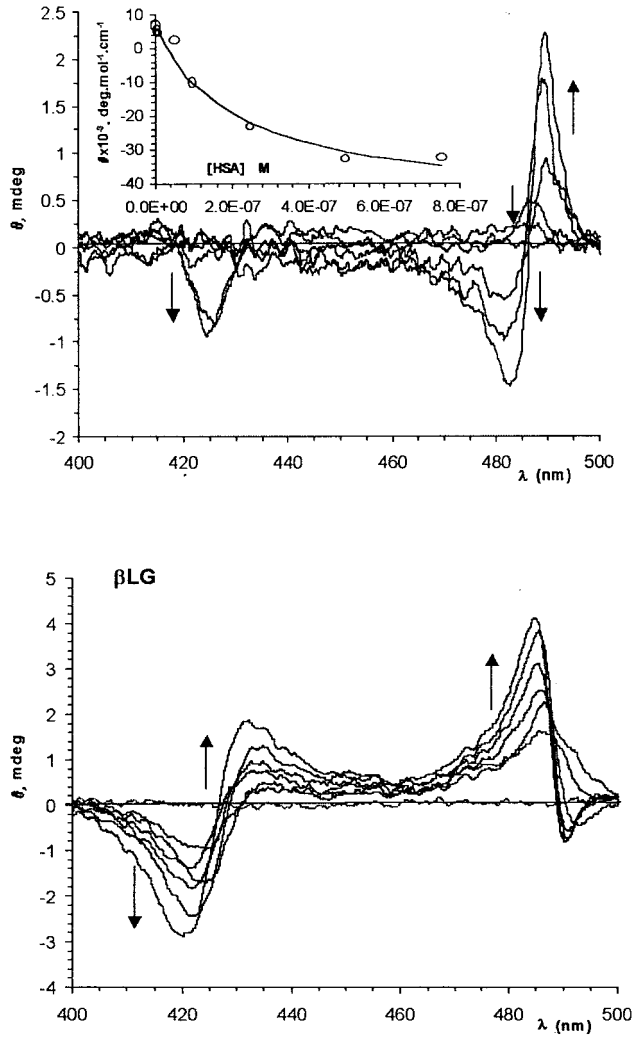

FIGURE 7 Induced CD spectra of TSPP (2 μM) by the presence of increasing concentration (indicated by the *arrows* sign) of HSA (*upper*) and βLG (*bottom*) at pH 2. (*Insert*) Variation of the molar ellipticity of TSPP obtained at 490 nm at different concentrations of HSA.

The CD signal appears initially near the 490-nm absorption maximum of J-aggregate but for higher [HSA] that signal diminishes and a CD dispersion is observed around 425 nm. Such behavior is similar to the findings observed on absorption but different from that reported (Ohno et al., 1993). Increasing pH, the CD signal at 490 nm disappears but the CD dispersion around 425 nm remains suggesting that it does not belong to the J-aggregate but rather to the monomer in a different chiral environment or to a different chiral species.

In the presence of βLG, more intense CD signals are obtained around 490 nm and 425 nm at pH 2 and 3.3. The differences found between the two proteins reveal different chiral environments (different orientations of the peptide chain relatively to the porphyrin plane). Also, a change in the pH of the solution from 2 to 3.3 caused a tremendous effect on CD spectra of TSPP with HSA in contrast to those with βLG. HSA is known to undergo a conformational transition producing two isomeric forms, the F form around pH 4 and the E form below pH 3.0 (Muzammil et al., 1999).

Thus, it seems that the aggregation process takes place in the protein framework rather than in free aqueous solution because it depends on the protein nature and concentration.

The CD signal on far-UV reflects largely the secondary structure of the protein and arises from the inherent chirality of the polypeptide chain. Native HSA is a globular protein that contains ≈66% α-helix conformation at pH 7, which seems to be kept at pH 2 (Muzammil et al., 1999). The presence of TSPP induces spectral changes (data not shown) namely a red shift of 4 nm and a decrease in the CD signal, indicating a certain loss of helicity probably caused by electrostatic interactions (Davis et al., 1996). In turn, βLG native conformation is essentially β-sheet (52 and 10% α-helix) (Papiz et al., 1986) characterized by an intense negative band centered at 216 nm. The presence of TSPP does not induce important changes apart from a small gradual broadening of that band reflecting some loss of β-sheet content.

Because the secondary structure of the protein seems to play a crucial role on the TSPP aggregation process, it is

TABLE 4 Bimolecular rate constants for dynamic and static quenching of HSA and βLG by acrylamide in aqueous solutions with different concentrations of at pH 2, using Stern-Volmer equation and a modified one, Eq. 5 (for βLG). (λ_{ex} = 295 nm and λ_{em} = 338 nm, T = 24.0°C)

	HSA		βLG	
[TSPP] μM	$k_q \pm 0.03 \times 10^{-9}$* ($M^{-1}$ s^{-1})	$V \pm 0.01$ (M^{-1})	$k_q \pm 0.05 \times 10^{-9}$* ($M^{-1}$ s^{-1})	$V \pm 0.05$ (M^{-1})
0	0.92	0.70	0.58	0.51
2	0.78	1.02	0.84	0.24
5	0.78	1.33	0.75	0.24
10	0.79	1.20	0.62	0.37
15	0.87	1.51	0.61	0.52
20	0.95	1.32	0.54	0.50
30	1.10	1.34	0.55	0.50

*$k_q = K_{sv}/\langle\tau_0\rangle$ where $\langle\tau_0\rangle$ is an average value.

interesting to follow the protein fluorescence in the presence of the porphyrin.

Protein quenching studies

Acrylamide is an excellent neutral quencher that is sensitive to exposure of Trp residues. The fluorescence quenching of Trp residues in HSA (Eftink and Ghiron, 1976; Chadborn et al., 1999) and in βLG (Eftink and Ghiron, 1984; Palazolo et al., 2000) have already been studied in free aqueous solution. An upward curvature in the Stern-Volmer plot using fluorescence intensity data has been identified with the existence of static contributions, similar to that of free tryptophan (Eftink and Ghiron, 1984) or *N*-acetyl-L- tryptophan (Eftink and Ghiron, 1984; Andrade and Costa, 2000) in an aqueous solution.

HSA

The slope of the Stern-Volmer plot for HSA at pH 2 was 3.26 M^{-1} in agreement to that reported in literature of 3.3 M^{-1} at pH 2.5, which compared with 17.0 M^{-1} for NATA (*N*-acetyl-L-tryptophanamide) or even for L-tryptophan alone, at pH 7 shows an ~sixfold lower value indicating that the Trp residue is not fully accessible to the quencher. A quenching sphere volume (V) of 0.70 M^{-1} was found to account for the static contribution in HSA, quite less than that of free NATA or free Trp (~1.2 M^{-1}, Andrade and Costa, 2000). If an indole ring is shielded by protein segments, the probability to find nearby a quencher molecule is small (Eftink and Ghiron, 1976). Therefore, V can also account for the Trp exposure to the protein surface. The value of 0.70 M^{-1} points to a location of the Trp residue within the protein matrix, because values of $V = 1.0$ M^{-1} have been reported for a fully exposed residue (Eftink and Ghiron, 1976).

The excited state decay was measured using a time-correlated single photon counting, which was best described by a double-exponential function at pH 2, $\tau_1 = 2.20$ ns (60%), and $\tau_2 = 5.19$ ns (40%). Because both lifetimes and preexponential factors are affected by acrylamide, an average lifetime was used to calculate the bimolecular quenching rate, k_q, which can only have a qualitative meaning. A value of 0.90×10^9 M^{-1} s^{-1} again indicates a relatively inaccessible Trp residue.

The presence of TSPP, at pH 2, yields an upward curvature, which were well fitted using the Stern-Volmer equation presented in the Data analysis section, over the range of 0 to 0.25 M of acrylamide (Fig. 8 *a*). These relatively high quencher concentrations do not seem to have significant effects on HSA conformation because no fluorescence shift was detected.

Both dynamic and static quenching processes of HSA by acrylamide are affected by the presence of TSPP. In fact, for [TSPP] < 10 μM, the dynamic process seems to be less effective than without TSPP the opposite occurring for the static process. Above that concentration, there is no apparent change of the static contribution and the dynamic quenching efficiency increases and is even greater than without TSPP.

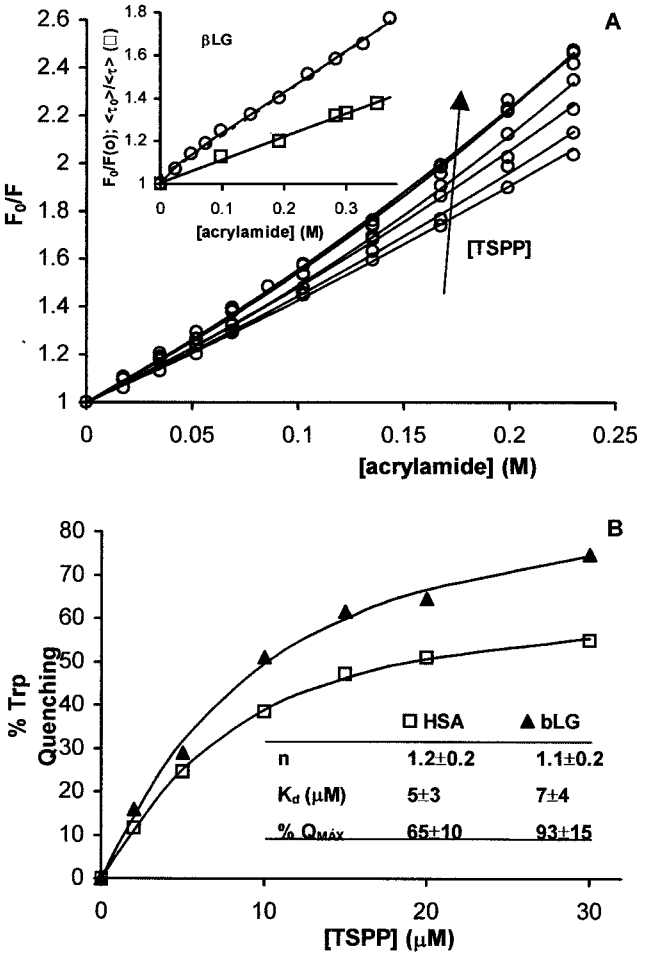

FIGURE 8 (*A*) Acrylamide quenching of the intrinsic Trp fluorescence of HSA (5 μM) in the presence of increasing TSPP concentrations (indicated by the *arrow* sign). Fit was achieved using Stern-Volmer equation to both steady- and transient-state data. Insert. Similar representation for βLG (5 μM) in the presence of TSPP (30 μM), fitted with Eq. 5. (*B*) Effect of TSPP binding on Trp intrinsic fluorescence of HSA (□) and βLG (▲). ($T = 24.0$°C, $\lambda_{ex} = 295$ nm, $\lambda_{em} = 338$ nm). Parameters were obtained by fit using Eq. 2.

The TSPP presence leads to a red-shift of the fluorescence spectra from 334 nm (HSA without TSPP, pH 2) to 338 nm in the presence of 30 μM TSPP.

HSA-TSPP

Binding of "substrates" to proteins can often cause quenching of the intrinsic Trp fluorescence. The addition of TSPP (2–30 μM) to HSA resulted in concentration-dependent quenching of Trp^{214} fluorescence, which reaches a plateau (Fig. 8 *b*). The intrinsic dissociation constant for binding, K_d, and the maximum quenching reached at saturation,

ΔF_{max}, can be estimated by fitting of the equation representing different binding sites with some degree of interaction (Eq. 2) to the quenching data giving good fittings. The errors and statistical significance were determined as described in the Data analysis section. The value of $K_d \approx 5.5$ μM is higher than that obtained previously by TSPP absorption after binding to HSA, $K_d = 1/K_b \approx 0.5$ μM. Although the Trp residue is sensitive to TSPP binding it does not quantitatively report the binding affinity. Fluorescence lifetime measurements were also performed at different TSPP concentrations showing a decrease in both components of the biexponential fitting below saturating concentration of the porphyrin.

βLG

Quenching by acrylamide leads to linear Stern-Volmer plots even in the presence of TSPP ≤ 15 μM. Above this concentration a downward curvature appears in the F_0/F plots (insert Fig. 8 *a*). In such a situation in which proteins contain more than one Trp residue each emitting independently, the proper equation is:

$$\frac{F_0}{F} = \left[\sum_{i=1}^{n} \frac{f_i}{(1 + K_i[Q])e^{V_i[Q]}}\right]^{-1} \quad (5)$$

in which K_i and V_i are the dynamic and the static quenching constants for each fluorescent component *i*, and f_i is its respective fractional contribution to the total fluorescence (Eftink and Ghiron, 1981).

The results obtained applying the former equation to both steady-state and transient-state data show that there are two type of Trp residues, one which is moderately accessible to acrylamide $k_{q1}(\text{eff}) \approx 0.62 \times 10^9$ M^{-1} s^{-1} ($k_q(\text{eff}) = K_{sv1} \times f_1/\tau_1$) and another that is almost inaccessible to collisions with the quencher ($k_q < 1 \times 10^7$ M^{-1} s^{-1}). The value of k_{q1} is comparable with that reported by Eftink and Ghiron (1984) at pH 4.5, 0.53×10^9 M^{-1} s^{-1}. The presence of TSPP seems to initially facilitate quenching by acrylamide, although for [TSPP] > 15 μM, a decrease in k_{q1} is obtained. Static quenching has also an important contribution especially for the less fluorescent contributing residues at higher [TSPP]. Nevertheless, the small changes found point to the inexistence of major conformational changes of βLG by the presence of TSPP.

βLG-TSPP

Similarly to HSA, the addition of TSPP (2–30 μM) to βLG also resulted in saturable concentration-dependent quenching of Trp fluorescence (Fig. 8 *b*), and a binding constant of 7.3 μM was found.

DISCUSSION

As mentioned before, TSPP is one of the few examples of molecules not belonging to the carbocyanine family that form pure J aggregates. Previous data concerning TSPP aggregation was achieved in the presence of high concentrations of cations including H^+ (Maiti et al., 1995, 1998), and in the presence of counter-charged surfactants, which were able, at low concentrations (below c.m.c.), to induce aggregation at a higher rate than cations (Maiti et al., 1998). Aggregation was also reported in confined media like aluminosilicate mesostructure (Xu et al., 2001) and adsorbed into polycation films (Van Patten et al., 2000) and TiO_2 nanoparticles (Yang et al., 2001). A common link may be established among them: all took place at low pH (≤ 3.5) when TSPP is a zwitterion and point to important electrostatic interactions. The strong Coulombic attraction between the positively charged macrocycles and the negatively charged sulfonate groups of neighboring molecules contribute to stabilize these J aggregates. Foremost, upon protonation TSPP is converted from a configuration in which the aryl moiety is twisted relative to the macrocycle plane to one in which it is nearly coplanar, in a fashion with a displacement between the next nearest neighbor such that oppositely charged sites are positioned closed to one another (head-to-tail alignment of the transition dipole moments).

The presence of HSA and βLG introduces remarkable changes in the spectroscopic features of TSPP. Both proteins possess positive global charge ($pI^{HSA} \approx 5.4$ (Dockal et al., 1999) and $pI^{\beta LG} \approx 5.2$ (Collini et al., 2000)) in acidic conditions. For instance, βLG has +20 charges at pH 2.0. So they may provide a positive microphase, distinct from the aqueous bulk, which induce TSPP aggregation in the presence of a submicromolar concentration of protein (a little higher for βLG whose positive charged residues may be less accessible to the porphyrin).

As more protein is added to the solution the balance between electrostatic and hydrophobic mutual interactions is such that J-aggregates are no longer stabilized and a complex TSPP-protein prevails. The Soret band of this complex shifts to the blue (for $TSPP^{2-}$) and to the red (for $TSPP^{4-}$) to a maximum around 420 nm in the presence of HSA, resembling that of TSPP in dimethylsulfoxide. This spectral shift is much less notorious in the presence of βLG ($\leq$3 nm), which seems to point to a more hydrophobic binding region on the HSA matrix while keeping an almost aqueous environment in the βLG binding location. This band at 420 nm has generated some controversy in the literature regarding its origin and was first assigned to an H aggregate-band, based on Raman data (Akins et al., 1994). This was ruled out due to Coulombic repulsion between the positively charged sulfonate groups (Maiti et al., 1995) and to CD spectroscopic features, which seemed to point to a common origin to the signals at 420 nm and 490 (Ohno et al., 1993). These authors supported the idea that H-dimers may be formed as intermediates in the J-aggregate process and in a more recent study, involving the interaction of TSPP with CTAB, they have only detected a weak CD

signal in the 490-nm region (Maiti et al., 1998). The latter findings are in agreement with our CD data reinforcing the idea that this maximum (at 420 nm) does not belong to the J-aggregate. Moreover, at pH 7 where no J-aggregates are detected, only a very weak CD signal is obtained exactly in the 420-nm region.

Time resolved fluorescence decays also indicate the existence of a common lifetime at the pH range studied ($\tau_f \approx$ 13 ns), which appears in the presence of any of two proteins and whose population grows with the increase of the protein concentration, therefore being associated with the TSPP-protein complex.

The dissociating constants obtained from absorption and/or fluorescence are more than 10 times higher than those reported for hemin binding at pH 7 to HSA ($K_d \approx 2 \times 10^{-8}$ M) and to βLG ($K_d \approx 2.5 \times 10^{-7}$ M) (Dufour et al., 1990). The metal presence in hemin could promote specific interactions with a disulphide bridge of the protein justifying the differences found. However, the same group reported a $K_d \approx 4 \times 10^{-7}$ M for the interaction between βLG and protoporphyrin IX, which is also a free-base porphyrin. These dissociating constants reflect a balance of a series of possible interactions ligand protein. In our study the K_d dependence on pH puts into evidence the existence of electrostatic interactions. Although studies indicate that for some ligands hydrophobic interactions may be stronger than the electrostatic forces in albumins, the latter must be significant because uncharged hydrocarbon chains have low binding affinity to the protein (Gelamo and Tabak, 2000).

At this stage, it is clearly necessary to look at the complex from the protein side. As it has been thoroughly emphasized, Trp fluorescence is highly sensitive to the polarity of its environment (Lakowicz, 1983), usually presenting a red shift in a more polar surrounding. Regarding HSA-TSPP interaction at pH 2, a double exponential fitting showed nearly invariance of preexponentials and a decrease in each lifetime, which reflects different solvent exposure of Trp^{214} in the various conformational substates. Both dynamic and static quenching rate constants indicate that Trp^{214} is not fully accessible to acrylamide in agreement with other reported data (Muzammil et al., 1999) but is extensively affected by the presence of TSPP.

The shift (from 334 to 338 nm) observed in the fluorescence spectra of Trp^{214} in the presence of TSPP, indicates an increase in the polar environment of the residue, which could be due to conformational changes induced by the porphyrin. This exposure would lead to an increase in k_q and V. As seen before, for higher ratios protein/porphyrin, a complex prevails, whereas for lower ratios the porphyrin tends to self-aggregate. So, while protein-porphyrin complex affects the Trp^{214} fluorescence that of the J-aggregate does not. The latter, due to the aggregate dimensions cannot assess the interior location of the Trp^{214} although it causes some conformational changes on the protein, making this residue more accessible to acrylamide. Nevertheless, the minor variations in k_q do not foresee major conformational changes, which is in agreement with the small differences found in far-UV CD spectra of HSA in the presence of TSPP.

Because there is an important overlap between Trp emission spectrum and TSPP absorption spectrum, the quenching may be associated with an energy transfer mechanism, an hypothesis reinforced with the appearance of the Trp residue absorption band in the fluorescence excitation spectrum of the complex. The type of energy transfer may be derived from R_0, the critical distance at which the rate of energy transfer is equal to the reciprocal of the donor fluorescence lifetime. The value of R_0 calculated for the Trp^{214}-TSPP complex was 56 Å, which suggests that the long distance Förster resonance energy transfer, is a possible mechanism to the observed quenching. The degree of quenching implies that TSPP binds to a site within the protein that can interact with the emitting Trp^{214} residue. If we take the TSPP-HSA complex to be nonspecifically bound to the surface of HSA (which is in agreement with data presented) a range of energy transfer efficiencies are expected. A crude estimate might be done based only in the protein dimensions $\sim 30 \times 80 \times 80$ Å (Das et al., 1999). Assuming that Trp^{214} and TSPP lie in opposite extremes of HSA, the energy transfer efficiency, $E = R_0^6/R_0^6 + R^6$), would be ≈98% at 30 Å and 11% at 80 Å. A location of TSPP molecules at a 10 Å center-to-center distance from Trp^{214} is unlikely because then only a negligible amount of fluorescence from this residue would be detected.

The three-dimensional structure of HSA is well characterized by x-ray crystallography with a resolution of 2.8 Å (He and Carter, 1992) and more recently with a resolution of 2.5 Å (Díaz et al., 2001). There are two binding sites of high affinity for small heterocyclic or aromatic compounds like warfarin or aspirin (located on subdomains IIA and IIIA) and another two dominant sites for long-chain fatty acids (IB and IIIB) and two distinct metal-binding sites. The location of Trp^{214} residue was assumed to be in a hydrophobic pocket of subdomain IIA, therefore its emission may be used to examine this domain. The other binding site in domain IIA lies within 10 Å distance from Trp^{214} (He and Carter, 1992). Both binding sites (IIA and IIIA) are structurally characterized by the presence of a buried hydrophobic cavity capped by charged and polar residues. Parr and Pasternack (1977) found no evidence that positively charged porphyrins like TMpyP and CoTMpyP bind to HSA. Nevertheless, TSPP binding is favorable at both ionic states (di-anion and tetra-anion) and a hydrophobic environment must be involved because the spectral shift is significant. All data obtained converge to a probable location of TSPP within such binding subdomains (IIA and/or IIIA) where the hydrophobic cavity would justify the spectral shifts and less accessibility to acrylamide sensed in the presence of the porphyrin, but close to Trp^{214} considering the effective energy transfer from that residue. Because

charged residues surround the binding site, conformational changes are expected upon pH increase and could account for the changes in the binding constants and on the CD spectra in both the far UV and visible region.

βLG appears to lack specificity for particular ligands and some studies suggest the existence of at least three independent binding sites (Sawyer et al., 1998). One is an internal site localized in the β-barrel of the protein, which can readily accommodate retinol and some fatty acids. The others are "surface" sites. From a recent review (Sawyer et al., 1998) it is possible to conclude that elongated ligands are favored in the barrel site.

The small changes found in TSPP spectra point to a preferential location on the "surface" sites. Moreover, recent studies suggest that there is a pH control of access to the interior of the calyx of βLG: the closed calyx characteristic of βLG at low pH, protects the ligand in the acidic stomach while the opened calyx, characteristic of βLG at high pH permits release of the ligand in the small intestine for absorption (Qin et al., 1998; Uhrínová et al., 2000). Because at pH 2 TSPP clearly senses the acidic environment, one is lead to assume that the porphyrin is not deep inside the calyx of the protein structure. On the other hand, the need of higher βLG concentration to achieve the same effect as that found with HSA could mean that TSPP has affinity for both binding sites populating also the more hydrophobic one. Thus, one would expect to find a spectral shift due to these interactions, which however do not occur.

The binding constants at increasing pH follow a sigmoidal trend with a "turning point" at pH 4.0. In a recent study (Collini et al., 2000), the pK value for the titration of the surface site was reported to be 4.0, whereas that for the internal site was 4.6, suggesting that Glu (glutamate) and Asp (aspartate) were the residues involved. At $pH < pK_a$, Glu and Asp residues are neutral and global positive charge prevail. On the other hand, above pK_a these residues become negative, and so the global charge on the protein turns negative. Several of these residues lie next to both the surface site and the β-barrel entrance. So, once again the most probable location for TSPP on βLG seems to be the surface site.

By contrast with HSA, βLG possess two tryptophan residues, Trp^{19} in an apolar environment lying only 3.0 to 4.0 Å from a guanidine group of Arg^{124} and Trp^{61} near the molecular surface but close to a disulfide bridge. Because both Arg and the disulfide bridge can be efficient quenchers of Trp fluorescence, some discrepancy has been found in literature as to which residue the βLG fluorescence can be attributed to (Brownlow et al., 1997; Palazolo et al., 2000).

The R value (≈100 Å), obtained from dynamic and static quenching data, shows that the energy transfer process is less efficient in this case, $E \approx 3\%$. This efficiency has to be looked upon as an average value for the two Trp residues, and taking into account R_o (≈56 Å) probably reflects a situation where only one of the residues contributes to an efficient energy transfer process.

CONCLUSIONS

Spectroscopic properties of a water soluble porphyrin, TSPP, with two carrier proteins, HSA and βLG, have common features but are differently dependent on the protein/porphyrin ratio. In both cases electrostatic interactions seem to play the major role. The interaction leads, for low concentrations of protein (submicromolar for HSA and micromolar for βLG) to the aggregation of TSPP classified as J-type, as detected by absorption, fluorescence, and CD. Increasing the protein concentration, a noncovalent TSPP-protein complex occurs but in different environmental sites of each protein studied. In the case of HSA that is likely to be in domain IIA or IIIA where its hydrophobic interior accounts for the spectral shift detected in spectra. As for βLG the absence of such a significant shift leads to envisage a "surface" binding site as the most probable, which is also supported by the strong dependence of the binding constants on pH and small changes in the far-UV CD of the protein.

Fluorescence quenching of Trp also confirms such "binding" locations and clearly puts into evidence a mechanism of energy transfer from Trp residue(s) to TSPP at pH 2.

This work was supported by Project POCTI/35398/QUI/2000. The authors thank Professor J. Costa Pessoa for the use of CD spectrometer. S. M. Andrade thanks FCT for the award of a BPD grant 18855.

REFERENCES

Akins, D. L., H.-R. Zhu, and C. Guo. 1994. Absorption and Raman scattering by aggregated meso-tetrakis(p-sulfonatophenyl)porphine. *J. Phys. Chem.* 98:3612–3618.

Andrade, S. M., and S. M. B. Costa. 2000. The location of tryptophan, *N*-acetyltryptophan and α-chymotrypsin in reverse micelles of AOT: a fluorescence study. *Photochem. Photobiol.* 72:444–450.

Avdulov, N. A., S. V. Chochina, V. A. Daragan, F. Schroeder, K. H. Mayo, and W. G. Wood. 1996. Direct binding of ethanol to bovine serum albumin: a fluorescent and ^{13}C NMR multiplet relaxation study. *Biochemistry.* 35:340–347.

Barteri, M., M. C. Gaudiano, S. Rotella, G. Benagiano, and A. Pala. 2000. Effect of pH on the structure and aggregation of human glycodelin A: a comparison with β-lactoglobulin A. *Biochim. Biophys. Acta.* 1479: 255–264.

Ben-Hur, E., and B. Horowitz. 1995. Advances in photochemical approaches for blood sterilization. *Photochem. Photobiol.* 62:383–388.

Bonnett, R. 1995. Photosensitizers of the porphyrin and phthalocyanine series for photodynamic theory. *Chem. Soc. Rev.* 24:19–33.

Borissevitch, I. E., T. T. Tominaga, H. Imasato, and M. Tabak. 1996. Fluorescence and optical absorption study of interaction of two water soluble porphyrins with bovine serum albumin: the role of albumin and porphyrin aggregation. *J. Luminesc.* 69:65–76.

Brownlow, S., J. H. M. Cabral, R. Cooper, D. F. Flower, S. J. Yewdall, I. Polikarpov, A. C. T. North, and L. Sawyer. 1997. Bovine β-lactoglobulin at 1.8 Å resolution: still an enigmatic lipocalin. *Structure.* 5:481–495.

Chadborn, N., J. Bryant, A. J. Bain, and P. O'Shea. 1999. Ligand-dependent conformational equilibra of serum albumin revealed by tryptophan fluorescence quenching. *Biophys. J.* 76:2198–2207.

Collini, M., L. D'Alfonso, and G. Baldini. 2000. New insight on β-lactoglobulin binding sites by 1-anilinonaphthalene-8-sulfonate fluorescence decay. *Prot. Sci.* 9:1968–1974.

Das, K., A. V. Smirnov, J. Wen, P. Miskovsky, and J. W. Petrich. 1999. Photophysics of hypericin and hypocrellin A in complex with subcellular components: interactions with human serum albumin. *Photochem. Photobiol.* 69:633–645.

Davila, J., and A. Harriman. 1990a. Photochemical and radiolytic oxidation of a zinc porphyrin bound to human serum albumin. *J. Am. Chem. Soc.* 112:2686–2690.

Davila, J., and A. Harriman. 1990b. Photoreactions of macrocyclic dyes bound to human serum albumin. *Photochem. Photobiol.* 51:9–19.

Davis, D. M., D. McLoskey, D. J. S. Birch, P. R. Gellert, R. S. Kittlety, and R. M. Swart. 1996. The fluorescence and circular dichroism of proteins in reverse micelles: application to the photophysics of human serum albumin and *N*-acetyl-tryptophanamide. *Biophys. Chem.* 60:63–77.

Díaz, N., D. Suárez, T. L. Sordo, and K. M., Merz Jr. 2001. Molecular dynamics study of the IIA binding site in human serum albumin: influence of the protonation state of Lys-195 and Lys-199. *J. Med. Chem.* 44:250–260.

Dockal, M., D. C. Carter, and F. Rücker. 1999. The three recombinant domains of human serum albumin. *J. Biol. Chem.* 274:29303–29310.

Dufour, E., M. C. Marden, and T. Haertlé. 1990. β-Lactoglobulin binds retinal, and protoporphyrin IX at two different binding sites. *FEBS Lett.* 277:223–226.

Eftink, M. R., and C. A. Ghiron. 1976. Exposure of tryptophanyl residues in proteins: quantitative determination by fluorescence quenching studies. *Biochemistry.* 15:672–680.

Eftink, M. R., and C. A. Ghiron. 1981. Fluorescence quenching studies with proteins. *Ann. Biochem.* 114:199–227.

Eftink, M. R., and C. A. Ghiron. 1984. Indole fluorescence quenching studies on proteins and model systems: use of the inefficient quencher succinimide. *Biochemistry.* 23:3891–3899.

Esposito, B. P., A. Faljoni-Alário, J. F. S. Meneses, H. F. Brito, and R. Najjar. 1999. A circular dichroism and fluorescence quenching study of the interactions between rhodium(II) complexes and human serum albumin. *J. Inorg. Biochem.* 75:55–61.

Figueiredo, T. L. C., R. A. W. Johnstone, A. M. P. Sørensen, D. Burget, and P. Jacques. 1999. Determination of fluorescence yields, singlet lifetimes and singlet oxygen yields of water-insoluble porphyrins and metalloporphyrins in organic solvents and in aqueous media. *Photochem. Photobiol.* 69:517–528.

Frapin, D., E. Dufour, and T. Haertlé. 1993. Probing the fatty acid binding site of β-lactoglobulin. *J. Prot. Chem.* 12:443–449.

Gelamo, E. L., and M. Tabak. 2000. Spectroscopic studies on the interaction of bovine (BSA) and human (HSA) serum albumins with ionic surfactants. *Spectrochim. Acta A.* 56:2255–2271.

Grossweiner, L. I., and G. C. Goyal. 1984. Binding of hematoporphyrin derivative to human serum albumin. *Photochem. Photobiol.* 40:1–4.

He, X. M., and D. C. Carter. 1992. Atomic structure and chemistry of human serum albumin. *Nature.* 358:209–215.

Huang, C. Z., Y. F. Li, K. A. Li, and S. Y. Tong. 1998. Spectral characteristics of the aggregation of α, β, γ, δ-tetrakis(*p*-sulfophenyl)porphyrin in the presence of proteins. *Bull. Chem. Soc. Jpn.* 71:1791–1797.

Lakowicz, J. R. 1983. Principles of Fluorescence Spectroscopy. Plenum Press, New York.

Lide, D. R. 1991. Appendix A: Mathematical Tables. *In* Handbook of Chemistry and Physics, 72nd Edition. D. R. Lide, editor-in-chief. CRC Press, Boca Raton, FL.

Maiti, N. C., S. Mazumdar, and N. Periasamy. 1998. J- and H- aggregates of porphyrin-surfactant complexes: time-resolved fluorescence and other spectroscopic studies. *J. Phys. Chem. B.* 102:1528–1538.

Maiti, N. C., M. Ravikanth, S. Mazumdar, and N. Periasamy. 1995. Fluorescence dynamics of noncovalent linked porphyrin dimers and aggregates *J. Phys. Chem.* 99:17192–17197.

Muzammil, S., Y. Kumar, and S. Tayyab. 1999. Molten-globule-like state of human serum albumin at low pH. *Eur. J. Biochem.* 266:26–32.

Nelson, S. W., C. V. Iancu, J.-Y. Choe, R. B. Honzatko, and H. J. Fromm. 2000. Tryptophan fluorescence reveals the conformational state of a dynamic loop in recombinant porcine fructose-1,6-bisphosphatase. *Biochemistry.* 39:11100–11106.

O'Connor, D. V., and D. Phillips. 1984. Time-correlated single photon counting. Academic Press, New York.

Ogoshi, H., and T. Mitzutani. 1998. Multifunctional and chiral porphyrins: model receptors for chiral recognition. *Acc. Chem. Res.* 31:81–89.

Ohno, O., Y. Kaizu, and H. Kobayashi. 1993. J-aggregate formation of a water-soluble porphyrin in acidic aqueous media. *J. Chem. Phys.* 99: 4128–4139.

Palazolo, G., F. Rodríquez, B. Farruggia, G. Picó, and N. Delorenzi. 2000. Heat treatment of β-lactoglobulin: structural changes studied by partitioning and fluorescence. *J. Agric. Food Chem.* 48:3817–3822.

Papiz, M. Z. L. Sawyer, E. E. Eliopoulos, A. C. T. North, J. B. C. Findlay, R. Sivaprasadarao, T. A. Jones, M. E. Newcomer, and P. J. Kraulis. 1986. The structure of β-lactoglobulin and its similarity to plasma retinal-binding protein. *Nature.* 324:383–385.

Parr, G. R., and R. F. Pasternack. 1977. The interaction of some water-soluble porphyrins and metalloporphyrins with human serum albumin. *Bioinorg. Chem.* 7:277–282.

Qin, B. Y., M. C. Bewley, L. K. Creamer, H. M. Baker, E. N. Baker, and G. B. Jameson. 1998. Structural basis of the Tanford transition of bovine β-lactoglobulin. *Biochemistry.* 37:14014–14023.

Saboury, A. A., A. K. Borbar, and A. A. Moosavi-Mavahedi. 1996. Resolution method of two sets of binding sites for the cationic surfactant-urease interaction. *Bull. Chem. Soc. Jpn.* 69:3031–3035.

Sawyer, L., S. Brownlow, I. Polikarpov, and S.-Y. Wu. 1998. β-Lactoglobulin: structural studies, biological clues. *Int. Dairy J.* 8:65–72.

Togashi, D. M., and S. M. B. Costa. 2000. Absorption, fluorescence and transient triplet-triplet absorption spectra of zinc tetramethylpyridylporphyrin in reverse micelles and microemulsions of aerosol OT–(AOT). *Phys. Chem. Chem. Phys.* 2:5437–5444.

Tominaga, T. T., V. E. Yushmanov, I. E. Borissevitch, H. Imasato, and M. Tabak. 1997. Aggregation phenomena in the complexes of iron tetraphenylporphine sulfonate with bovine serum albumin. *J. Inorg. Biochem.* 65:235–244.

Tsuchida, T., G. Zheng, R. K. Pandey, W. R. Potter, and D. A. Bellinier. 1997. Correlation between site II-specific human serum albumin (HSA) binding affinity and murine in vivo photosensitising efficacy of some photofrin components. *Photochem. Photobiol.* 66:224–228.

Uhehara, K., Y. Hioki, and M. Mimuro. 1993. The chlorophyll *a* aggregate absorbing near 685 nm is selectively formed in aqueous tetrahydrofuran. *Photochem. Photobiol.* 58:127–132.

Uhrínová, S., M. H. Smith, G. B. Jameson, D. Uhrín, L. Sawyer, and P. N. Barlow. 2000. Structural changes accompanying pH-induced dissociation of the β-lactoglobulin dimer. *Biochemistry.* 39:3565–3574.

Van Patten, P. G., A. P. Shreve, and R. J. Donohoe. 2000. Structural and photophysical properties of a water-soluble porphyrin associated with polycations in solution and electrostatically-assembled ultrathin films. *J. Phys. Chem. B.* 104:5986–5992.

Xu, W., H. Guo, and D. L. Akins. 2001. Aggregation of tetrakis(*p*-sulfonatophenyl)porphyrin within modified mesoporous MCM-41. *J. Phys. Chem. B.* 105:1543–1546.

Yang, X., Z. Dai, A. Miura, and N. Tamai. 2001. Different back electron transfer from titanium dioxide nanoparticles to tetra (4-sulfonatophenyl)porphyrin monomer and its J-aggregate. *Chem. Phys.Lett.* 334:257–264.